

Study of single-nucleon transfer reactions in the $^{18}\text{O}+^{48}\text{Ti}$ collision at 275 MeV

O. Sgouros^{1,2,}, F. Cappuzzello^{1,2}, M. Cavallaro¹, D. Carbone¹, C. Agodi¹, G. A. Brischetto^{1,2}, D. Calvo³, E. R. Chávez Lomeli⁴, I. Ciraldo^{1,2}, M. Cutuli^{1,2}, G. De Gregorio^{5,6}, F. Delaunay^{1,2,7}, H. Djapo⁸, C. Eke⁹, P. Finocchiaro¹, M. Fisichella¹, A. Gargano⁵, M. A. Guazzelli¹⁰, A. Hacisalihoglu¹¹, R. Linares¹², J. Lubian¹², N. H. Medina¹³, M. Morales¹⁴, J. R. B. Oliveira¹³, A. Pakou¹⁵, L. Pandola¹, V. Soukeras^{1,2}, G. Souliotis¹⁶, A. Spatafora^{1,2}, D. Torresi¹, A. Yildirim¹⁷, and V. A. B. Zagatto¹²* for the NUMEN collaboration

¹INFN – Laboratori Nazionali del Sud, Catania, Italy

²Dipartimento di Fisica e Astronomia "Ettore Majorana", Università di Catania, Catania, Italy

³INFN - Sezione di Torino, Torino, Italy

⁴Instituto de Física, Universidad Nacional Autónoma de México, Mexico City, Mexico

⁵INFN - Sezione di Napoli, Napoli, Italy

⁶Dipartimento di Matematica e Fisica, Università della Campania "Luigi Vanvitelli", Caserta, Italy

⁷LPC Caen UMR6534, Université de Caen Normandie, ENSICAEN, CNRS/IN2P3, Caen, France

⁸Ankara University, Institute of Accelerator Technologies, Turkey

⁹Department of Mathematics and Science Education, Akdeniz University, Antalya, Turkey

¹⁰Centro Universitario FEI, São Bernardo do Campo, Brazil

¹¹Department of Physics, Recep Tayyip Erdogan University, Rize, Turkey

¹²Instituto de Física, Universidade Federal Fluminense, Niterói, Brazil

¹³Instituto de Física, Universidade de São Paulo, São Paulo, Brazil

¹⁴Instituto de Pesquisas Energeticas e Nucleares IPEN/CNEN, São Paulo, Brazil

¹⁵Department of Physics, University of Ioannina and HINP, Ioannina, Greece

¹⁶Department of Chemistry, University of Athens and HINP, Athens, Greece

¹⁷Department of Physics, Akdeniz University, Antalya, Turkey

Abstract. The study of single-nucleon transfer reactions for the $^{18}\text{O}+^{48}\text{Ti}$ system was pursued at the energy of 275 MeV as part of a more systematic study which is undertaken within the NUMEN and NURE experimental campaigns. The aim is to measure the complete set of available reaction network which are characterized by the same initial and final-state wavefunctions as the more suppressed double charge exchange reactions. Understanding the degree of competition between successive nucleon transfer and double charge exchange reactions is crucial for the description of the meson-exchange mechanism. In this respect, angular distribution measurements for one- and two-nucleon transfer reactions for the $^{18}\text{O}+^{48}\text{Ti}$ system were carried out at the MAGNEX facility of INFN-LNS in Catania. An overview of the data analysis for the $^{48}\text{Ti}(^{18}\text{O},^{19}\text{F})^{47}\text{Sc}$ and $^{48}\text{Ti}(^{18}\text{O},^{17}\text{O})^{49}\text{Ti}$ reactions will be presented.

*e-mail: ououfrios.sgouros@lns.infn.it

1 Introduction

The interest of the Physics community in the neutrinoless double beta ($0\nu\beta\beta$) decay is kept vivid through the years. An observation of such a rare decay would confirm the hypothesis of Majorana that neutrinos are their own anti-particles and would allow us to determine the absolute mass scale of the neutrino, providing the decay rate and the nuclear matrix elements (NMEs). However, the NMEs for this process are a piece of the puzzle, since their calculation relies on different nuclear structure models and is susceptible to large uncertainties. For this purpose, high quality experimental data are necessary to provide the appropriate constraints on the theoretical models.

The NUMEN (NUclear Matrix Elements for Neutrinoless double beta decay) project [1] consists of a seminal experimental campaign undertaken at INFN-LNS which proposes a new experimental approach to obtain data-driven information on the NMEs of the $0\nu\beta\beta$ decay. That is to use double charge exchange (DCE) reactions induced by heavy ions for a variety of $0\nu\beta\beta$ decay candidate targets. In this context, the ^{48}Ti nucleus is of great interest since it is the daughter nucleus of ^{48}Ca in the $\beta\beta$ decay process [2]. The choice of DCE reactions as probes for studying the $0\nu\beta\beta$ decay stems from the fact that, despite some differences, the two processes probe the same initial and final-state nuclear wavefunctions [1, 3]. Furthermore, it was recently shown that the NMEs of these two processes can be directly linked, under specific conditions [3, 4].

In general, the DCE mechanism consists of three possible reaction modes: The direct meson-exchange DCE reaction [5–7], the double single charge exchange reaction (DSCE) [8] and the multi-nucleon transfer reactions [9–15]. All these reaction pathways may in principle populate the same final states, but only the first is directly connected to the $0\nu\beta\beta$ decay. However, since all three reaction modes are experimentally indistinguishable, it is very important to quantify possible contributions from DSCE and/or multi-nucleon transfer to the measured DCE cross-sections [15], which may be the key for accessing the information of the NMEs of the $0\nu\beta\beta$ decay [3, 7].

Taking into consideration all the above, in the present work which is part of the NURE project [16], the $^{18}\text{O}+^{48}\text{Ti}$ collision was studied by measuring in the same experiment the complete set of the available reaction channels that may contribute to the $^{48}\text{Ti}\rightarrow^{48}\text{Ca}$ transition. The present contribution provides an overview of the analyses of the $^{48}\text{Ti}(^{18}\text{O},^{19}\text{F})^{47}\text{Sc}$ one-proton and $^{48}\text{Ti}(^{18}\text{O},^{17}\text{O})^{49}\text{Ti}$ one-neutron transfer reactions [17, 18]. The analyses of other reaction channels are ongoing [19, 20].

2 Experimental details

The experiment was performed at the MAGNEX facility [21, 22] of INFN-LNS in Catania. The $^{18}\text{O}^{8+}$ ion beam was delivered by the K800 Superconducting Cyclotron at the energy of 275 MeV with an intensity of few enA and impinged on a TiO_2 target evaporated on a thin ^{27}Al foil. In this respect, supplementary measurements with a self-supporting ^{27}Al target and a WO_3 target with an aluminium backing were carried out, under the same experimental conditions, for estimating the background contributions originating from the reaction of the $^{18}\text{O}^{8+}$ beam with the aluminum backing and the oxygen component of the compound target.

The various reaction ejectiles were momentum analyzed by the MAGNEX large acceptance magnetic spectrometer [21, 22]. MAGNEX is a high-performance optical spectrometer comprised of a large aperture quadrupole lens followed by a dipole bending magnet, capable of detecting from very light [23] up to heavy ions [24] preserving a high energy, mass and angular resolution. The optical axis of the spectrometer was set at $\theta_{opt}=9^\circ$ with respect to the beam axis, while its angular acceptance was delimited by four slits located ~ 250 mm

downstream of the target position. Thus, the explored angular range included angles between 3° and 15° in the laboratory reference frame.

Having crossed the spectrometer, the ions were detected by the MAGNEX Focal Plane Detector (FPD) [25], located ~ 200 cm downstream at the exit of the dipole bending magnet. The FPD comprises a gas detector followed by a wall of 60 silicon detectors to measure the ion residual energy ($E_{res.}$). The use of this gas detector is twofold. It serves as a proportional drift chamber for measuring the energy loss of the ions in the gas (ΔE), but also as a position-sensitive detector for measuring the horizontal and vertical positions and angles of the ion tracks. In this way, the reconstruction of the ejectile paths inside the spectrometer may be performed. Furthermore, by using the information provided by the FPD, the particle identification (PID) was performed following the prescription reported in Ref. [26]. As a first step, using the well-known $\Delta E - E$ technique the different ions were discriminated based on their atomic number. Subsequently, the different isotopes of the same ion family were identified adopting a technique which is based on the correlation between kinetic energy and the measured horizontal position of the ions at the focal plane. Examples of PID spectra for single-proton and single-neutron transfer reactions are reported in Refs. [17, 19].

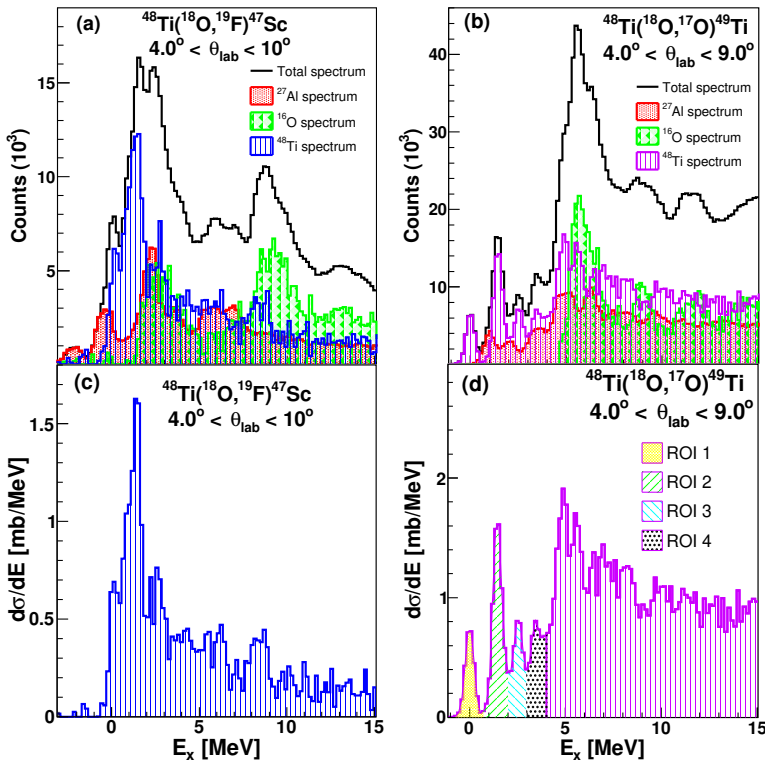


Figure 1. Experimental data for the (left) one-proton and (right) one-neutron transfer reactions at 275 MeV. In panels (a) and (b) the decomposition of the excitation energy spectra for the one-proton and one-neutron transfer reactions, respectively, is shown. Panels (c) and (d) illustrate the energy distributions for the one-proton and one-neutron transfer reaction, respectively. In the latter, the legend indicates the regions of interest for which angular distribution data were determined. Figures are taken from Refs. [17, 18].

3 Data reduction and results

After the PID was completed, a software trajectory reconstruction was applied to the data in order to obtain the momentum vector of the ions at the target position [27]. In this procedure, having determined the phase space parameters (horizontal and vertical positions and angles) at the focal plane of the spectrometer, the equation of motion for each of the identified particles was solved up to the 10th order using the COSY INFINITY code [28], the ion path through the spectrometer was reconstructed and subsequently, the scattering parameters of the ion at the target position were determined (e.g. kinetic energy, scattering angle). The excitation-energy spectrum was determined as $E_x = Q_0 - Q$, where Q_0 is the ground state (g.s.) to g.s. Q -value and Q is the reaction Q -value calculated adopting the missing-mass method [21] assuming two-body kinematics. The obtained excitation energy spectra are shown in the panels (a) and (b) of Fig. 1 for the $^{48}\text{Ti}(^{18}\text{O}, ^{19}\text{F})^{47}\text{Sc}$ and the $^{48}\text{Ti}(^{18}\text{O}, ^{17}\text{O})^{49}\text{Ti}$ reactions, respectively. As it was already mentioned, a titanium oxide target with an aluminum backing was used. Therefore, the measured spectrum was contaminated with events coming from the interaction of the beam with the different target materials. However, having performed supplementary measurements using a self-supporting aluminum target and an oxygen one, it was possible to subtract the background yields and obtain the energy spectrum for the reactions of interest. The background subtraction procedure for the single-proton and single-neutron transfer reactions is visualized in Fig. 1 (a) and (b), respectively. After subtracting the background yields, by taking into account the integrated beam charge during the acquisition time, the scattering centers of the titanium target, the solid angle and the efficiency of the spectrometer, absolute energy-differential cross-sections for both reactions were deduced and are presented in the panels (c) and (d) of Fig. 1.

The energy resolution in similar measurements is ~ 500 keV FWHM [17]. In Refs. [17, 18] a relevant discussion on the statistical and systematic uncertainties is given. This, in conjunction with the high density of states of ^{47}Sc nucleus in the $^{48}\text{Ti}(^{18}\text{O}, ^{19}\text{F})^{47}\text{Sc}$ reaction, gives rise to an almost continuous energy distribution, while a sharp increase in the magnitude of cross-section at $E_x \sim 1.5$ MeV is ascribed to the excitation of ^{19}F to the $(\frac{5}{2}^+)_1$ state at 0.197 MeV, with ^{47}Sc populating the $(\frac{3}{2}^+)_1$ and $(\frac{1}{2}^+)_1$ states at 0.767 MeV and 1.391 MeV, respectively. To this extent, the experimental yields over a wide excitation energy region, namely $0 \leq E_x \leq 3.5$ MeV, were integrated in steps of $\Delta\theta_{lab.} = 0.5^\circ$ to extract angle-differential cross-sections which are shown in Fig. 2 (a). As regards the $^{48}\text{Ti}(^{18}\text{O}, ^{17}\text{O})^{49}\text{Ti}$ reaction, its energy distribution manifests some pronounced structures corresponding to various states of the ejectile and the recoil nuclei. Also, due to a slightly better energy resolution for this reaction channel (~ 400 keV FWHM), the region of interest (ROI) 1 in Fig. 1 (d) which corresponds to the g.s. to g.s. transition is well-separated from the rest of the observed structures. On the same footing as before, the experimental yields for each ROI were integrated over each angular slice to obtain angle-differential cross-sections. As a representative case, the angular distribution data corresponding to ROI 3 are presented in Fig. 2 (b).

The measured cross-sections were analyzed within the distorted-waves and coupled-channels Born approximation (DWBA and CCBA) frameworks using the FRESKO code [29]. In both calculations, the optical potentials in the entrance and exit channels were described in a double-folding approach adopting the São Paulo potential [30]. The validity of the entrance channel potential was checked against elastic scattering data [20] which were measured in the same experiment as the present single-nucleon transfer reactions. The spectroscopic amplitudes for the projectile and target overlaps were calculated with large-scale shell-model calculations using the KSHELL code [31]. In more details, the calculation of the spectroscopic amplitudes for the projectile overlaps, namely the $\langle ^{19}\text{F} | ^{18}\text{O} \rangle$ and $\langle ^{17}\text{O} | ^{18}\text{O} \rangle$ ones, were performed adopting the p-sd-mod [32] interaction. Instead, for the target

overlaps, namely the $\langle ^{47}\text{Sc} | ^{48}\text{Ti} \rangle$ and $\langle ^{49}\text{Ti} | ^{48}\text{Ti} \rangle$ ones, the spectroscopic amplitudes were derived using the SDPF-MU interaction [33]. In this context, theoretical calculations were performed for the single-nucleon transfer reactions and are compared to the data in Fig. 2.

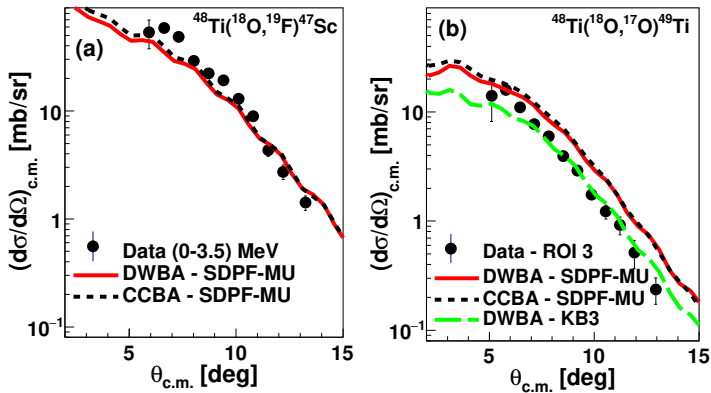


Figure 2. Angular distribution data for the (a) one-proton and (b) one-neutron reactions at 275 MeV. The experimental data, indicated by the black points, are compared to the results of DWBA and CCBA calculations which are depicted with the colored curves. Figures are taken from Refs. [17, 18].

For the $^{48}\text{Ti}(^{18}\text{O}, ^{19}\text{F})^{47}\text{Sc}$ reaction, the experimental data are described adequately-well by the theoretical calculations. The result of the CCBA calculation is similar to that obtained with the DWBA approach suggesting that the involved states are characterized by a substantial single-particle strength. Furthermore, the very good agreement between experimental data and theory supports the validity of the adopted optical potentials for the description of the elastic scattering in the entrance and exit channels and also confirms the shell-model description of the involved nuclei. As regards the $^{48}\text{Ti}(^{18}\text{O}, ^{17}\text{O})^{49}\text{Ti}$ reaction, it can be seen that the theoretical prediction overestimates the experimental data by a factor of ~ 2 . This discrepancy is attributed to a large cross-section predicted for the $(\frac{5}{2}^-)_3$ state of the ^{49}Ti nucleus, associated to the larger value of the predicted spectroscopic amplitude compared to (d,p) experiments [34]. This hypothesis is further corroborated by the results of a tentative shell-model calculation adopting the KB3 interaction, where a smaller value of the spectroscopic amplitude for this state is predicted. Using the results of this new calculation, it can be seen that the agreement between data and theory is significantly improved. This result points to some deficiency of the SDPF-MU interaction which seems to require a modification of the single-neutron strength distribution for the $(\frac{5}{2}^-)_3$ state of ^{49}Ti with respect to the KB3 interaction. A detailed description of the data interpretation can be found elsewhere [17, 18].

4 Summary

A multi-channel study of the $^{18}\text{O}+^{48}\text{Ti}$ collision at 275 MeV was performed as part of the NUMEN and NURE projects, aiming at measuring the complete set of the available direct reactions. Angular distribution measurements for the reaction ejectiles were performed at the MAGNEX facility of INFN-LNS. The present work summarizes the main findings from the analyses of the one-proton and one-neutron transfer reactions. The experimental differential cross-sections were found to be in good agreement with the theoretical calculations. Especially for the case of the $^{48}\text{Ti}(^{18}\text{O}, ^{17}\text{O})^{49}\text{Ti}$ one-neutron transfer reaction, an appreciable

sensitivity of the differential cross-sections on different nuclear structure models was found. Such a result highlights transfer reactions as the best tool for identifying the most appropriate nuclear structure model for the description of the many-body nuclear wavefunctions of the interacting nuclei. Furthermore, this result provides an important input to the analysis of the DCE reaction, underlining that special attention should be given to the choice of the nuclear structure model for an accurate description of the wavefunctions of the involved nuclei, with major consequences in the determination of the NMEs for the $\beta\beta$ decay process.

Acknowledgments. This project has received financial support from the European Research Council (ERC) under the European Union's Horizon 2020 Research and Innovation Programme (NURE - Grant agreement No. 714625).

References

- [1] F. Cappuzzello *et al.*, Eur. Phys. J. A **54**, 72 (2018)
- [2] A. Belley *et al.*, Phys. Rev. Lett. **126**, 042502 (2021)
- [3] H. Lenske *et al.*, Prog. Part. Nucl. Phys. **109**, 103716 (2019)
- [4] E. Santopinto *et al.*, Phys. Rev. C **98**, 061601(R) (2018)
- [5] F. Cappuzzello *et al.*, Eur. Phys. J. A **51**, 145 (2015)
- [6] V. Soukeras *et al.*, Results in Physics **28**, 104691 (2021)
- [7] F. Cappuzzello *et al.*, Prog. Part. Nucl. Phys. **128**, 103999 (2023)
- [8] M. Cavallaro *et al.*, 2021 Front. Astron. Space Sci. **8**, 659815 (2021)
- [9] D. Carbone *et al.*, Phys. Rev. C **102**, 044606 (2020)
- [10] J. L. Ferreira *et al.*, Phys. Rev. C **103**, 054604 (2021)
- [11] S. Calabrese *et al.*, Phys. Rev. C **104**, 064609 (2021)
- [12] I. Ciraldo *et al.*, Phys. Rev. C **105**, 044607 (2022)
- [13] S. Burrello *et al.*, Phys. Rev. C **105**, 024616 (2022)
- [14] A. Spatafora *et al.*, Phys. Rev. C **107**, 024605 (2023)
- [15] J. L. Ferreira *et al.*, Phys. Rev. C **105**, 014630 (2022)
- [16] M. Cavallaro *et al.*, PoS **BORMIO 2017**, 015 (2017)
- [17] O. Sgouros *et al.*, Phys. Rev. C **104**, 034617 (2021)
- [18] O. Sgouros *et al.*, Phys. Rev. C **108**, 044611 (2023)
- [19] O. Sgouros, Il Nuovo Cimento **45 C**, 70 (2022)
- [20] G. A. Brischetto *et al.*, Submitted for publication in Phys. Rev. C
- [21] F. Cappuzzello *et al.*, Eur. Phys. J. A **52**, 167 (2016)
- [22] M. Cavallaro *et al.*, Nucl. Instrum. Methods Phys. Res. B **463**, 334 (2020)
- [23] A. Pakou *et al.*, Eur. Phys. J. A **57**, 25 (2021)
- [24] G. A. Souliotis *et al.*, Nucl. Instrum. Methods Phys. Res. A **1031**, 166588 (2022)
- [25] D. Torresi *et al.*, Nucl. Instrum. Methods Phys. Res. A **989**, 164918 (2021)
- [26] F. Cappuzzello *et al.*, Nucl. Instrum. Meth. A **621**, 419 (2010)
- [27] F. Cappuzzello *et al.*, Nucl. Instrum. Methods Phys. Res. A **638**, 74 (2011)
- [28] K. Makino *et al.*, Nucl. Instrum. Methods Phys. Res. A **427**, 338 (1999)
- [29] I. J. Thompson, 1988 Comput. Phys. Rep. **7**, 167 (1988)
- [30] M. A. Candido Ribeiro *et al.*, Phys. Rev. Lett **78**, 3270 (1997)
- [31] N. Shimizu *et al.*, Comput. Phys. Commun. **244**, 372 (2019)
- [32] Y. Otsuno *et al.*, Phys. Rev. C **83**, 021301(R) (2011)
- [33] Y. Otsuno *et al.*, Phys. Rev. C **86**, 051301(R) (2012)
- [34] A. E. Ball *et al.*, Nucl. Phys. A **183**, 472 (1972)